Journal of Engineering and Applied Sciences 10 (3): 45-57, 2015
ISSN: 1816-949X

Cavitation Noise Characterization of Two B-series Propeller Models in the Cavitation Tunnel

[1, 2]Endang Widjiati, [2]Eko Budi Djatmiko, [2]Wisnu Wardhana and [3]Wirawan
[1]Indonesia Hydrodynamic Laboratory, UPT BPPH-BPPT, 60111 Surabaya, Indonesia
[2]Department of Ocean Engineering, [3]Department of Electrical Engineering,
Institut Teknologi Sepuluh Nopember, 60111 Surabaya, Indonesia

Abstract: Analysing characteristics of propeller cavitation noise is necessary in relation with the identification of noise signature in conjunction with both surface ship and submarine operations. Since, the noise signature is determined by propeller, flow and machinery noise then any vessel that has certain propeller, hull shape and machines will have a peculiar signature. The propeller cavitation noise can be generated by means of experiment performed in a cavitation tunnel. This study reports some results of the noise characterization experiment conducted in the Cavitation Tunnel available at the Indonesian Hydrodynamic Laboratory, Surabaya, Indonesia. Two B-series propeller models, i.e., 4 and 7-blade were studied in the experiment. Time-Frequency distribution, namely Wigner-Ville Distribution (WVD) is applied to observe the characteristics of the cavitation noise. Results show that the WVD can differentiate whether the propeller cavitation noise is generated either by the 4 or 7-blade propeller. In this study, three different kinds of categories in the appearance of cavitation are distinguished, i.e., when the propeller does not experience cavitation, if only hub and tip vortex cavitation develop and when various cavitations occur simultaneously.

Key words: Propeller cavitation noise, Wigner-Ville Distribution, vortex, simultaneously, Indonesia

INTRODUCTION

Studies on propeller cavitation noise have been done previously by several researchers for many years. Works done by Grenie (1990) and Zhang *et al*. (2007) are a few examples of work made in this field. In this respect, frequencies, duration, amplitudes and its spectra were studied and analyzed to prove the characteristics of the propeller cavitation noise as shown by Collier (1997). Since, the noise of one type of propeller might be different with another, this noise can be used for detecting and identifying type of surface ship or submarine that uses a certain kind of propeller. Therefore, these works can be applied for many applications where propeller cavitation noise involves.

To be able to get the propeller cavitation noise, Araki *et al*. (1982), Sharma *et al*. (1990) and Park *et al*. (2009) generate the occurrence of the propeller noise by using cavitation tunnel. In the tunnel, water flows and pressures can be customized as well as propeller rotation. As the propeller environment in the tunnel can be customized, the propeller cavitation noise can then be produced. The noise that appears is then recorded and studied further. Widjiati *et al*. (2012a) reports the spectrum characteristics of the propeller noise produced by the 4-blade B-series propeller.

Another work reported by Widjiati *et al*. (2012b) applies the Wigner-Ville Distribution (WVD) to identify the occurrence of propeller cavitation noise generated by a 4-blade propeller, since it can give a high resolution signal in a time-frequency domain. The WVD is used to differentiate whether the signal contains cavitation, just starts to have a cavitation or without cavitation. A 3D plot of the WVD can show clearly the transient signal occuring in the noise signal. Therefore, this technique is used for sonar and radar signal analysis. Since, the contour distribution of each type of signal can be identified, the occurrence of cavitation can therefore be detected from its own contour.

PROPELLER CAVITATION NOISE

When a ship is moving, there is an acoustic noise develops originating from the vessel. This acoustic noise comprises of three components, i.e., machinery noise, flow noise and propeller noise (Ross, 1987). The machinery noise is mainly initiated by the vibrations of the ship engine, the flow noise comes from interaction between

Corresponding Author: Endang Widjiati, Indonesia Hydrodynamic Laboratory, UPT BPPH-BPPT, 60111 Surabaya, Indonesia

the hull of moving ship and the water. The propeller noise is classified into two categories, i.e., the noise caused by the cavitation and that of non-cavitating condition (Carlton, 2007). There are three components of non-cavitating noise, i.e., tonal mechanical blade noise associated to the number of blades, broadband noise related to blade vibrations and the so called singing noise related to vortex shedding and blade resonant frequencies (Collier, 1997). The non-cavitationg noise will not be further discussed here.

Cavitation noise: According to Ross (1987) and Carlton (2007), the propeller cavitation noise is a major component of the vessel noise. Figure 1 shows an example of contribution of each component of the vessel noise as function of vessel speed. Figure 1 indicates the propeller cavitation noise dominates the vessel noise, especially at high speed. However, in lower speed, the flow noise (in figure shown as the boundary layer noise) will be larger in comparison to other components.

Carlton (2007) identifies that the propeller cavitation noise is generated by the collapse of cavitation bubbles. The more bubbles appear, the more radiated acoustic energy is dispersed because the bubbles and its collapse occur randomly (Carlton, 2007). The power spectral density experiences from the bubbles and its collapse are similar to the product of the number of bubbles per unit time and the spectral energy density due to the growth and collapse of a single bubble.

Moreover, Carlton (2007) stated that the process of cavitation starts when the bubbles are carried in the water flow because the fluid pressure decreases to the vapor pressure. The bubbles generate vibration and lead to a noisy sound when they burst and collide with the propeller. The more bubbles form and burst, the louder the noise will be. The cavitation also affects a decrease in efficiency of the propeller since it causes the onset of erosion on the propeller blades.

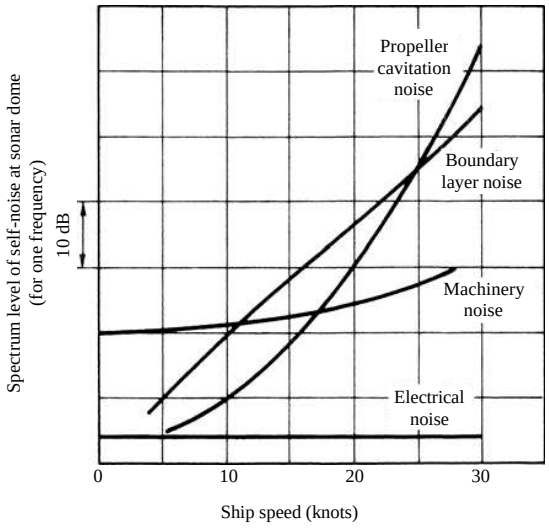

Fig. 1: Example of contribution of each components of vessel noise (Carlton, 2007)

Different references might give different type of classification of propeller cavitation noise. However, the type of cavitation can be categorized based on its location as shown in Fig. 2, namely blade tip, blade root (at the gap between hub and propeller blades), hull vortex cavitation, cloud cavitation, bubble cavitation and hub vortex cavitation (Carlton, 2007). Blade tip cavitation consits of the tip vortex cavitation and the sheet cavitation. The tip and root cavitation appear at the tip of propeller blade and propeller root, respectively where the pressure is relatively low.

By using a stroboscopic lighting equipment which has an adjustable light flashing speed, the cavitation appearance on the propeller can be clearly seen and observed (Carlton, 2007). The flashing light has to be set at the same speed as the rotation of the propeller. Example of the propeller cavitation phenomena captured using the photograph and the light originating from the stroboscope flash is given in Fig. 3. Figure 3 shows clearly both the tip cavitation and the hub vortex

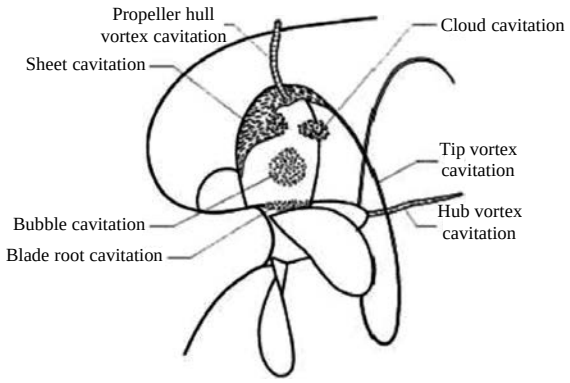

Fig. 2: Different types of cavitation [boatdesign.net]

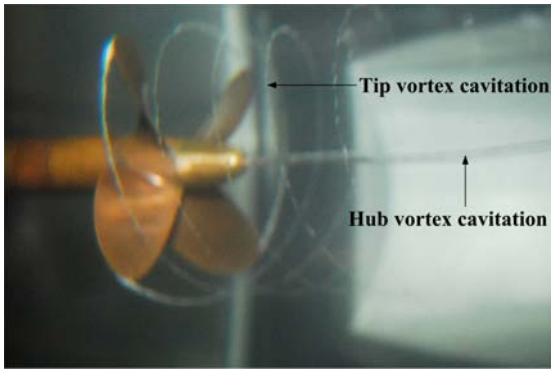

Fig. 3: Tip and hub vortex cavitation phenomena

cavitation. The first cavitation takes place during the experiment is the hub vortex cavitation, emerging at the hub of the propeller. The next cavitation arising is the tip cavitation which occurs at each end of the propeller blades and forms the twisted lines with the number of lines corresponding to the number of the propeller blades. During the test, it is observed that the louder the noise is brought about the more and the larger cavitations so exist. While the tip cavitation and other cavitations can only be seen clearly by using the stroboscope, the hub vortex cavitation can be clearly observed directly at the window of the measurement section of the cavitation tunnel.

Since, the propeller cavitation noise is dominant for a surface ship and submarine, this noise can be used for detection and/or identification of the ship class or the submarine class which usually has a certain type of propeller. Therefore, propeller cavitation noise will be further analyzed and used in the process for detection and identification of surface ship and submarine. This is planned for the future works.

Cavitation tunnel: In the researches done by Park *et al.* (2009) and Sharma *et al.* (1990), the cavitation tunnel was used to generate the propeller cavitation. Based on these papers, Widjiati *et al.* (2012a, b) used the cavitation tunnel at the Indonesian Hydrodynamic Laboratory (IHL), Surabaya, Indonesia to perform a set of experiments. In the work reported in this study, the same tunnel, i.e., the K16B-type cavitation tunnel is utilized. The water velocity and the pressure in this tunnel are varied to be able to produce different types of cavitation at different conditions. The cavitation tunnel is also equipped with a dynamometer that is functioned to hold and rotate the model propeller in the tunnel at different propeller rotation speed. The cavitation tunnel has an impeller which is in Fig. 4 located at the bottom on the right handside, functioned as the motor to run the water in the tunnel at certain velocity. Other dimensions of the tunnel parts are also given in Fig. 4. The measurement section of the cavitation tunnel, located at the top of the tunnel has a length of 4000 mm and a transverse section of a square shape sized 850 mm. The dynamometer is placed in the tunnel through the window at the top of this section that can be opened.

The propeller cavitation noise characteristics of two B-series propellers, i.e., the 4 and 7 blades are investigated. The profile view and projected outline with size and dimensions of these propeller models are exhibited in Fig. 5. The 4-blade propeller has a diameter of 234.5 mm and the 7-blade propeller has a diameter of 180 mm, AE/A0 of 0.7, P/D of 0.7 and pitch of 126 mm. The cavitation noise of these propellers are generated in different tunnel conditions, basically by varying the pressure and the water velocity inside the tunnel as well as the propeller rotation.

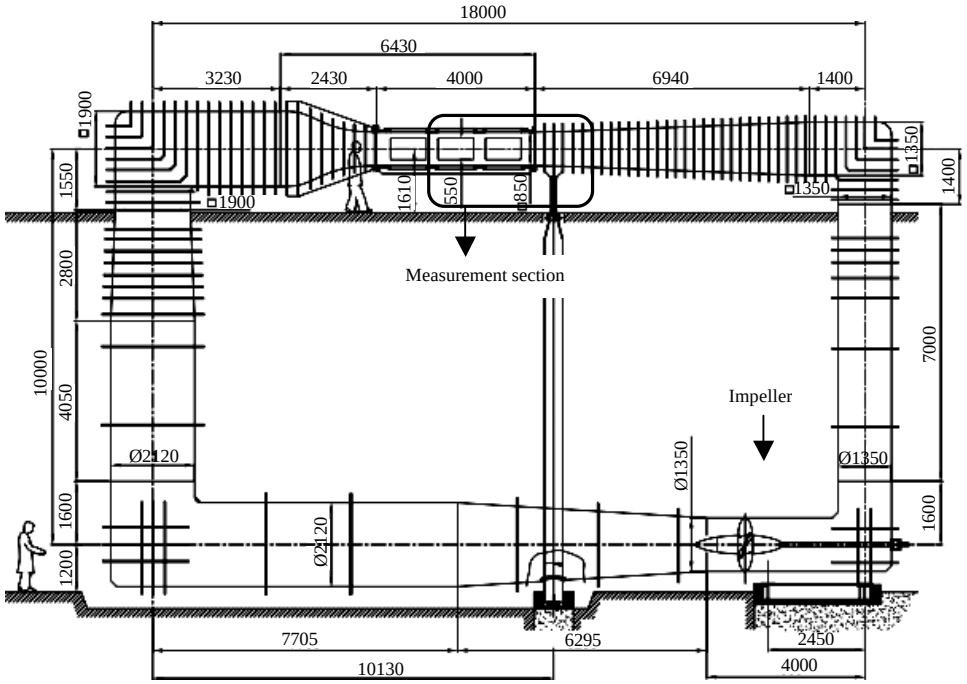

Fig. 4: Schematic diagram of the IHL cavitation tunnel (all dimensions are in mm)

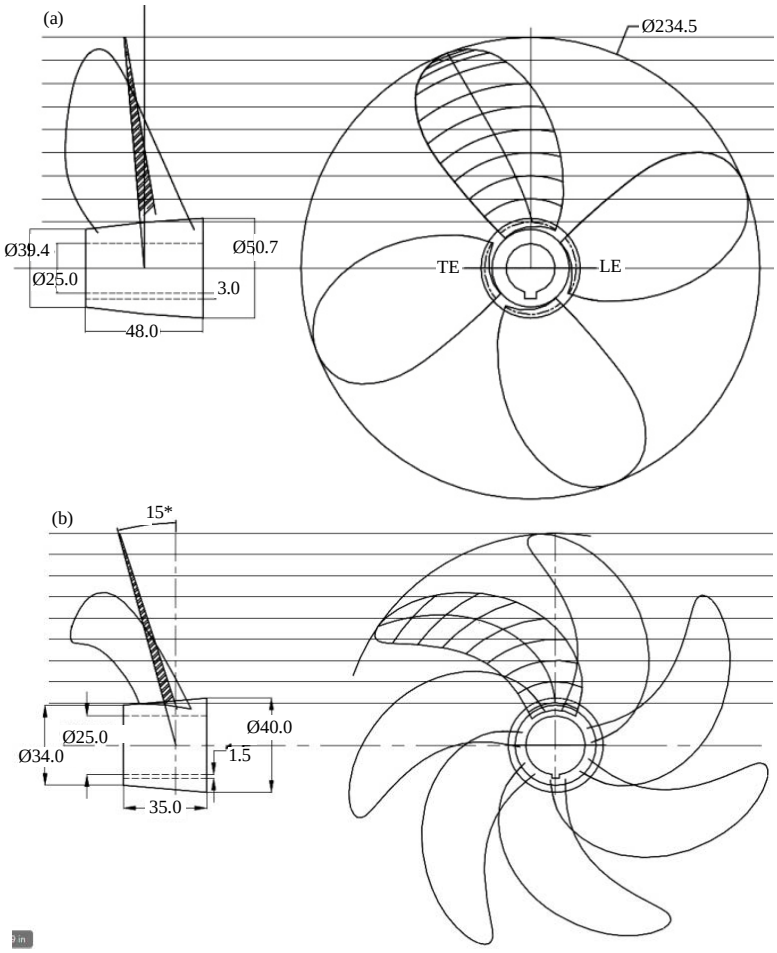

Fig. 5: a, b) Profile view and projected outline of the two propellers model tested (all dimensions are in mm)

MEASUREMENT PROCESSES

Figure 6 shows the configuration of an acoustic noise signal measurement which consits of a hydrophone and its preamplifier connected to the NI DAQ Card through the connector block. The acoustic noise signal so received is then recorded and displayed at the monitor using Labview. A single hydrophone is placed on one of the window lids of the measurement section of the cavitation tunnel at a distance of about 50 cm from the model propeller. This H2a-XLR Aquarian hydrophone with frequency range between 10-100 kHz is connected to the Rolls MP13 Mini Mic preamplifier that operates to activate the phantom power. The output of the preamplifier becomes the input for the NI PCI 6143 DAQ Card through the connector block. To distinguish the occurrence of the propeller cavitation during the experiment, a stand alone camera video recorder is utilized. It is expected that by observing both the measurement results and the video recordings of the phenomenon, in-depth understanding of the physical mechanism and characteristics of noises generated by the two propellers in various conditions can be investigated.

Three different pressures inside the tunnel are set during measurement, respectively 1.0, 1.4 and 1.8 bars. These conditions are meant to simulate the depth where the object is located in the real sea. The propeller rotation and the water flow velocity are other parameters that are adjusted in generating the propeller cavitations. In an actual vessel, the propeller rotation is initiated by the main engine while the water flow velocity represents the average velocity of the vessel in the water. The dynamometer of this cavitation tunnel can rotate the propeller up to 40 rps and this tunnel is also capable to handle the water flow velocity up to 12 m sec^{-1}. In these experiments, the propeller cavitation is imposed by rotating the propeller with velocity varied in the range of 1.0-29 rps with interval of 6.0-7.0 rps and flowing the water with the speed from 0.8-3.5 m sec^{-1} with an interval of 0.25-0.5 m sec^{-1}. By applying the variations of these

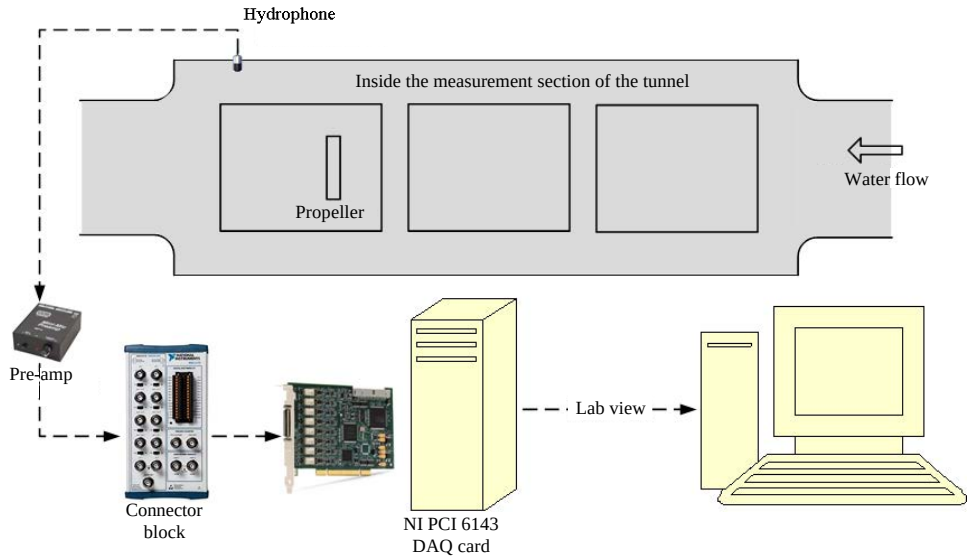

Fig. 6: Measurement scheme

variables, the occurrence of the propeller cavitation phenomena can be generated and observed for different values of the pressure in the tunnel, the speed of water flow and the propeller rotation speed. The existence of video recording during the experiment makes it possible to visually observe the appearance of propeller cavitation. Based on the measurement method described above, there are two assessments were then made. The first assessment is based on the visual observation whereas the second assessment is derived from the acoustic noise signal recorded during the experiments. Based on visual observation, Table 1 presents the summary of the occurrence of the propeller cavitation at different pressures (P) and water velocity for the 4 and 7-blade B-series propellers at the propeller rotation of 22 and 29 rps, respectively. Both for the 4 and 7-blade propeller models, the cavitation does not appear at rotation speed of 1 and 7 rps and for the 4-blade propeller and the small hub cavitation starts to arise only at the propeller rotation of 15 rps and the water speed of 3.0 and 3.3 m sec^{-1} at P = 1 bar. For the 4-blade propeller, the two different rotation speeds given in Table 1 are those where the propeller cavitation occurs at all three different pressures. For the 7-blade propeller, the cavitation never arises at the pressures of 1.4 and 1.8 bar while small hub cavitation and tip vortex cavitation occur at the pressure of 1.0 bar and the water velocity of 0.8 and 1.6 m sec^{-1}, respectively.

With reference to Table 1, for the 4-blade propeller, various cavitations occur simultaneously mostly at the propeller rotation of 29 rps. Figure 7 represents these condition where various cavitations occur, i.e., tip and hub vortex cavitations, sheet cavitation, bubble cavitation and cloud cavitation. In contrast with Fig. 3 which shows only the hub and tip vortex cavitations.

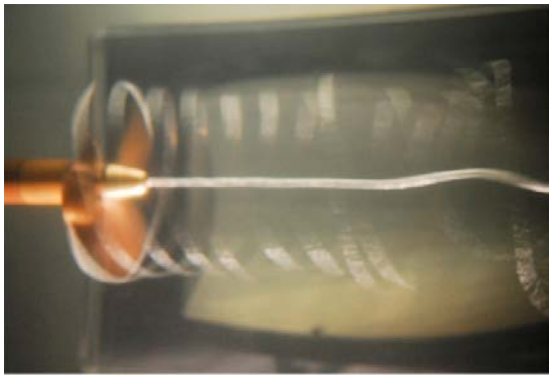

Fig. 7: Complex interaction of various types of propeller cavitation

Table 1: The occurence of cavitation

	4-blade						7-blade	
	P = 1 bar		P = 1.4 bar		P = 1.8 bar		P = 1 bar	
Water speed (m sec^{-1})	22	29	22	29	22	29	22	29
0.8	C	c	ht	c	h	c	h	ht
1.6	C	c	ht	c	h	c	h	ht
2.4	Ht	c	h	c	h	c	n	n
3.0	H	c	h	c	n	ht	n	n
3.3	H	c	n	ht	n	ht	n	n

n: no cavitation; h: hub cavitation; ht: hub and tip vortex cavitation; c: all types of cavitation

The second assessment derived from the acoustic noise signal recorded during the experiments is shown in Fig. 8-11. Figure 8-10 illustrate the amplitudes of the propeller noise for the 4-blade B-series propeller recorded at pressures of 1.0, 1.4 and 1.8 bar, respectively. While Fig. 11 shows the amplitude of the propeller noise for the 7-blade B-series propeller at pressures of 1.0 bar. Further,

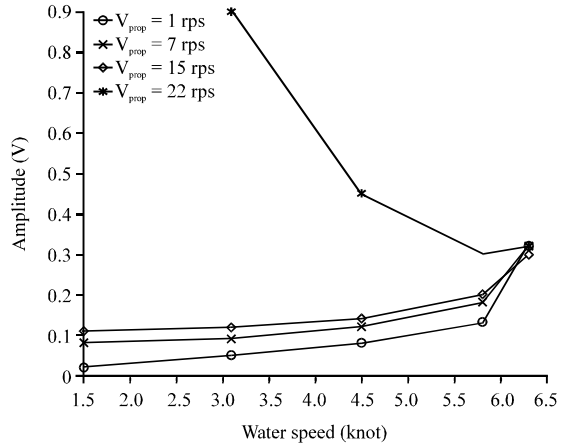

Fig. 8: Amplitude range of propeller noise for B-series 4-blade propeller at P = 1.0 bar for various propeller velocities

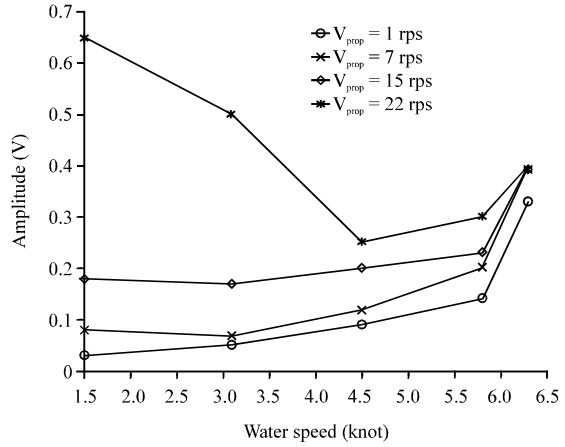

Fig. 9: Amplitude range of propeller noise for B-series 4-blade propeller at P = 1.4 bar for various propeller velocities

to the aforementioned observations, an analysis has been performed to obtain amplitude of the acoustic noise as presented below.

Comparing Table 1 to Fig. 8 and 9, it is proven that for the condition where large cavitation exists, the amplitude of the acoustic signal becomes very high. The trend of the acoustic signal amplitude is completely different when there is no cavitation or only small hub cavitation occurs. In every pressure condition, the trends of the noise amplitude for the propeller rotation below 22 rps are similar that is becoming larger with the increasing of water velocity. However, it is not the case when the propeller rotation is 22 rps where the cavitation occurs at low velocity that causes a high amplitude. This shows that the propeller cavitation noise has an amplitude acoustic

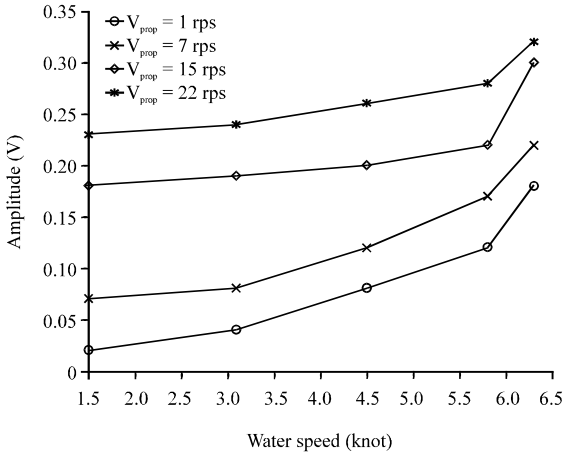

Fig. 10: Amplitude range of propeller noise for B-series 4-blade propeller at P = 1.8 bar for various propeller velocities

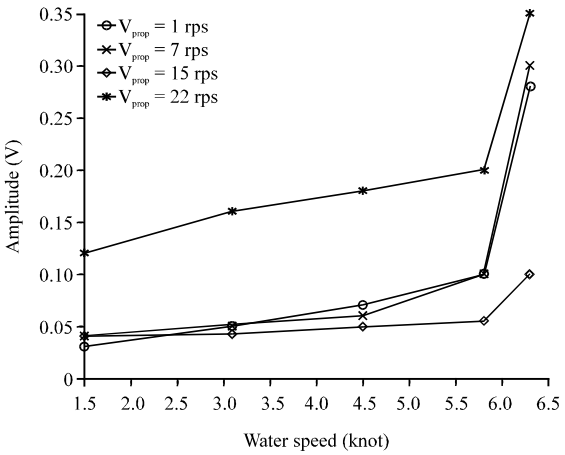

Fig. 11: Amplitude range of propeller noise for B-series 7-blade propeller at P = 1.0 bar for various propeller velocities

signal up to 0.9 V. Figure 10 proves also that the amplitude of the propeller noise will be <0.35 V when there is no cavitation or only small cavitation occurs.

Figure 11 shows the amplitude of the propeller noise signal recorded during the experiment at one condition using the B-series 7-blade propeller model in the cavitation tunnel. Comparing Fig. 11 with Table 1, it can be presumed that small cavitations do not affect the amplitude of the noise signal. It is small for low speed and become large for higher speed. Since, the characteristics of the noise signal can not be seen from its amplitude then the time-frequency analysis is used for this purpose as described in the next study.

WIGNER-VILLE DISTRIBUTION

Wigner-Ville Distribution (WVD) is the time and frequency distribution which can exactly show the frequency components of the signal both in time and frequency domain. The time-frequency distribution can be used for showing the frequency components of the signal at a constant-t section as well as the time or times where the frequency component exists (Boashash, 2003). Given this characteristic, the WVD is widely used to analyse a multi-component signal which is usually difficult to be shown, since it has some interferences among its components that make it difficult to read and analyze.

Figure 12 shows an example of the linear FM signal where the time-domain representation is given at the top part of the figure. Its spectrum is given in Fig. 12 in the box at the left part. Based on these two representations, both in the time domain or the frequency domain, the occurrence in time and frequency content is shown. Therefore, the WVD can be applied for this purpose. The plot at the center of Fig. 12 shows how the signal looks like in time and frequency domain. The Time-Frequency Distribution (TFD) using the WVD can show the frequency range and its start and stop times as well as the variation in frequency with time. Based on this characteristic, the WVD is used to analyze the propeller cavitation noise originated from the B-series 4 or 7-blade propeller.

The WVD of the signal x(t) denoted by W_x (t, f) is defined by the Wigner Distribution (WD) associated with its analytical form. The WVD equation can be written as:

$$W_z(t, f) = \underset{\tau \to f}{F}\left\{ z\left(t+\frac{\tau}{2}\right) z^*\left(t-\frac{\tau}{2}\right)\right\} \quad (1)$$

where, z(t) is the analytic associate of x(t). An analytical signal is a signal with Fourier transform that does not contain negative frequencies. Equation 1 shows that the WVD is a quadratic form distribution that computes a local time-frequency energy.

As mentioned in the study, the experiment starts with measuring the noise generated by the empty cavitation tunnel which means that the propeller is not placed in the tunnel yet. The acoustic noise in the tunnel when only the cooling fan is on at the high position is recorded and then further used as the noise reference of the cavitation tunnel system. The WVD representation of the recorded signals of this condition is shown in Fig. 13.

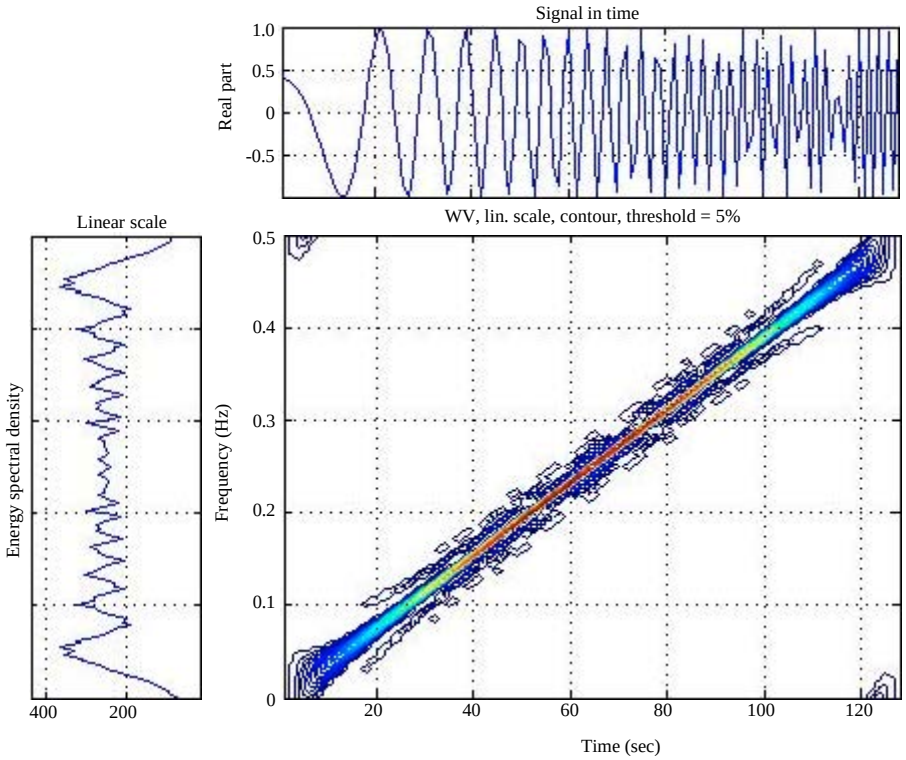

Fig. 12: Example of Wigner-Ville distribution representation of the linear FM signal

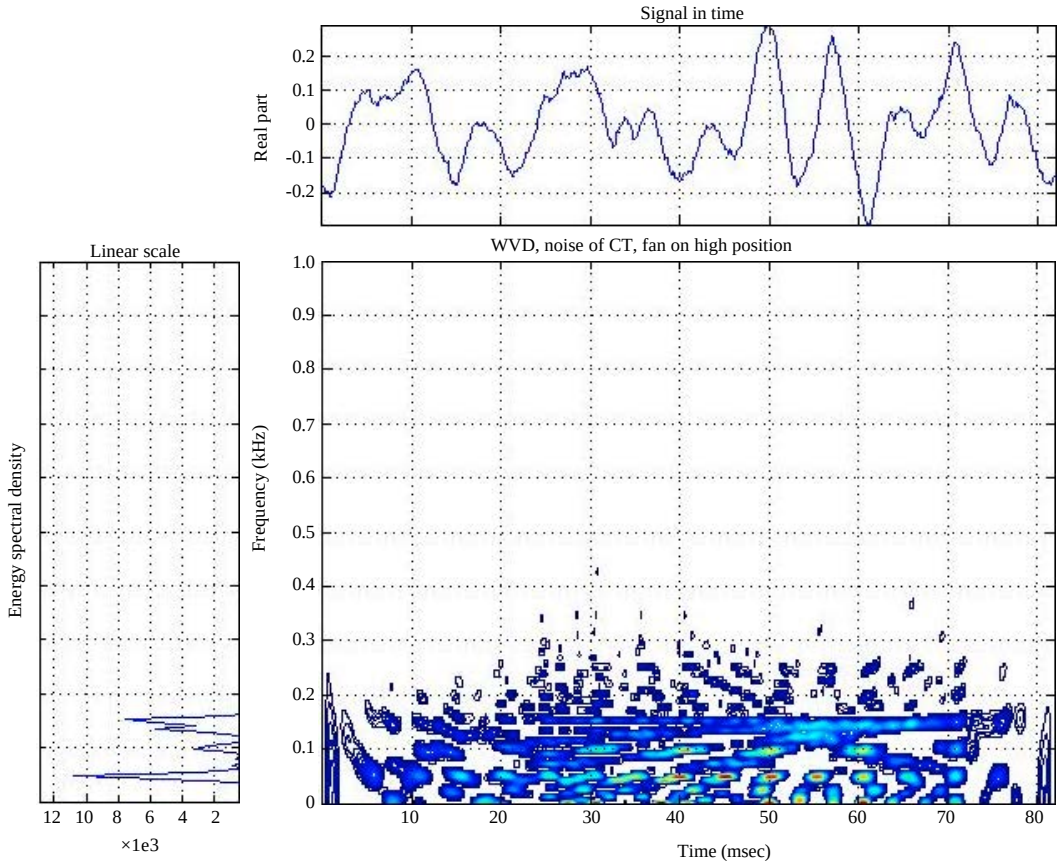

Fig. 13: The WVD representation of the acoustic noise in the tunnel when the cooling fan is on at the high position: a) V_{prop} = 22 rps and b) V_{prop} = 29 rps

Figure 13 indicates that the signal has low frequency components below 300 Hz. The highest energy signal lies at about 50 Hz which means that this frequency is generated by the acoustic noise originated by the high position of the cooling fan.

RESULTS

With reference to Table 1, different WVD representations of the experiment conditions at water speed of 3.1 knot, are presented in the following few figures. Figure 14a and b exhibit the WVD representations of the propeller noise, when more than one component of cavitation occur. Referring to Fig. 2, in this condition not only hub and tip vortex cavitation appears here but also cloud cavitation, sheet cavitation and bubble cavitation. These cavitations induce a noise level that is higher in comparison with the conditions given in Fig. 15a and b in which only two components of cavitation appear. The more cavitation components appear, the higher noise level becomes.

Figure 15a shows the WVD representation of the propeller noise when only the hub vortex and the tip vortex cavitation appear during the experiment. Moreover, Fig. 15b represents the condition when only the hub vortex cavitation starts to arise. Therefore, Fig. 14 and 15 demonstrate that the more cavitation components occur, the WVD representation shows a denser part in the middle. This event cannot be seen by only looking at the energy spectral density as given at the left part of each figure. The energy spectral density given in Fig. 14a shows that there are a few frequency components between 0.8-2.1 kHz which are the frequency components of the cavitation acoustic signal. These components do not occur in the energy spectral density of Fig. 15b, since the cavitation component that appears here is only the hub vortex cavitation. However, the frequency components between 1.6-2.1 kHz shown in Fig. 15a are not the frequency components of other types of cavitations, since it appears that more cavitation components occur in Fig. 14b. The frequency component of the cavitation noise originated from the cavitation components in

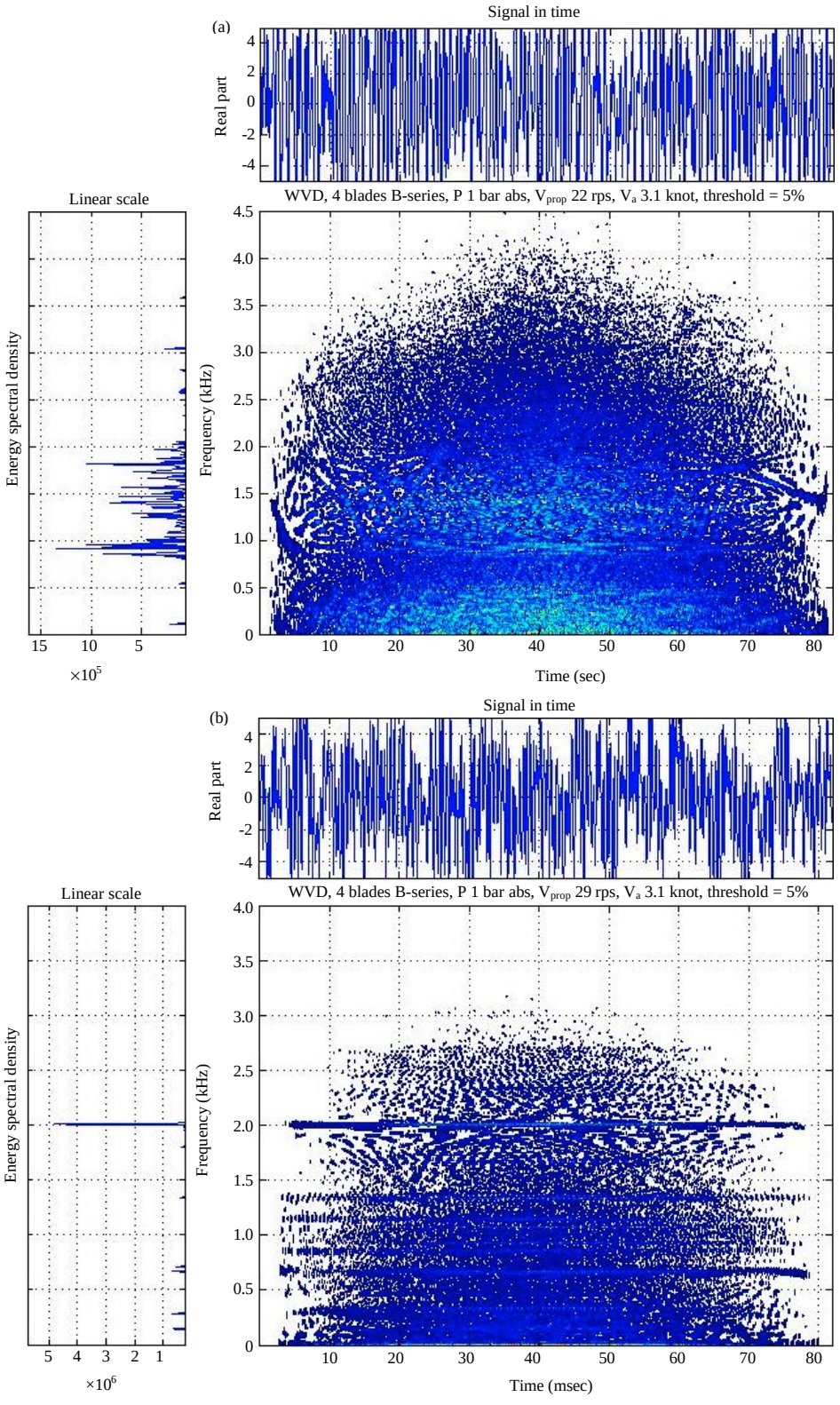

Fig. 14: The WVD representation of the acoustic noise in the tunnel when B-series 4-blade propeller rotates at $V_{water\ in\ the\ tunnel}$ = 3.1 knot and $P_{in\ the\ tunnel}$ = 1.0 bar: a) $P_{in\ the\ tunnel}$ = 1.4 bar b) $P_{in\ the\ tunnel}$ = 1.8 bar

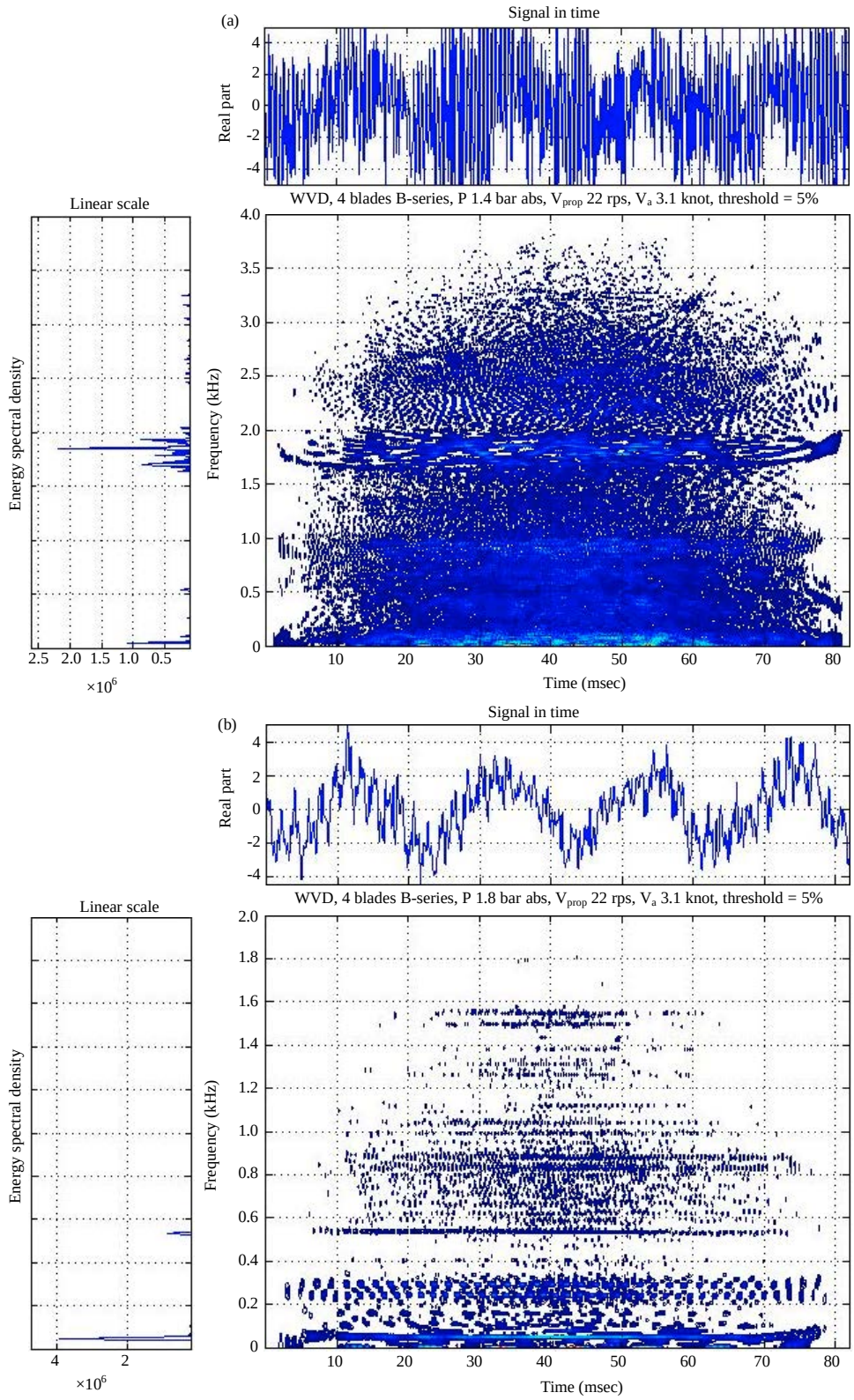

Fig. 15: The WVD representation of the acoustic noise in the tunnel when B-series 4-blade propeller rotates at 22 rps, $V_{\text{water in the tunnel}}$ = 3.1 knot: a) Propeller rotates at 22 rps and b) propeller rotates at 29 rps

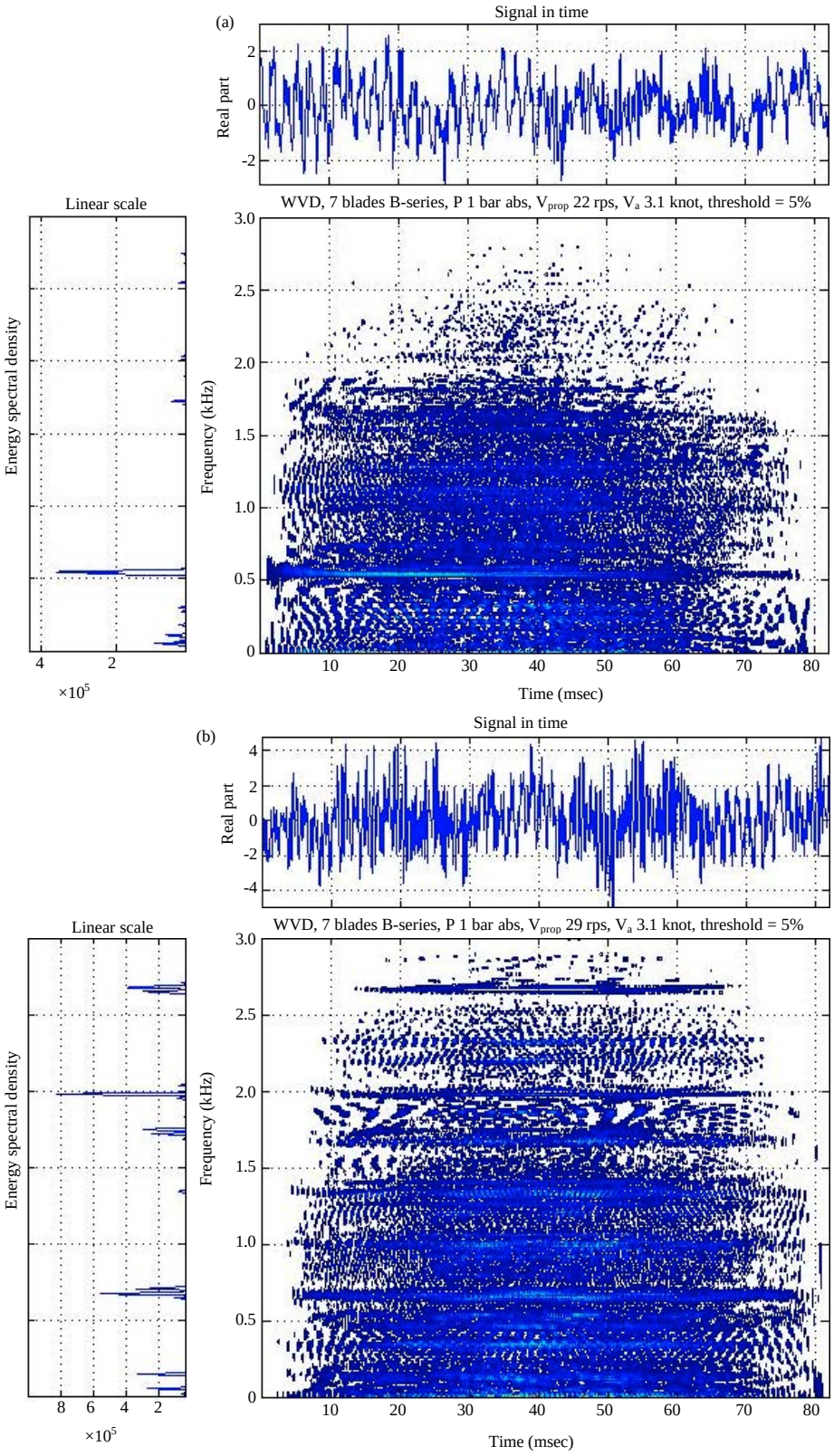

Fig. 16: The WVD representation of the acoustic noise in the tunnel when B-series 7-blade propeller, $V_{\text{water in the tunnel}}$ = 3.1 knot and $P_{\text{in the tunnel}}$ = 1.0 bar

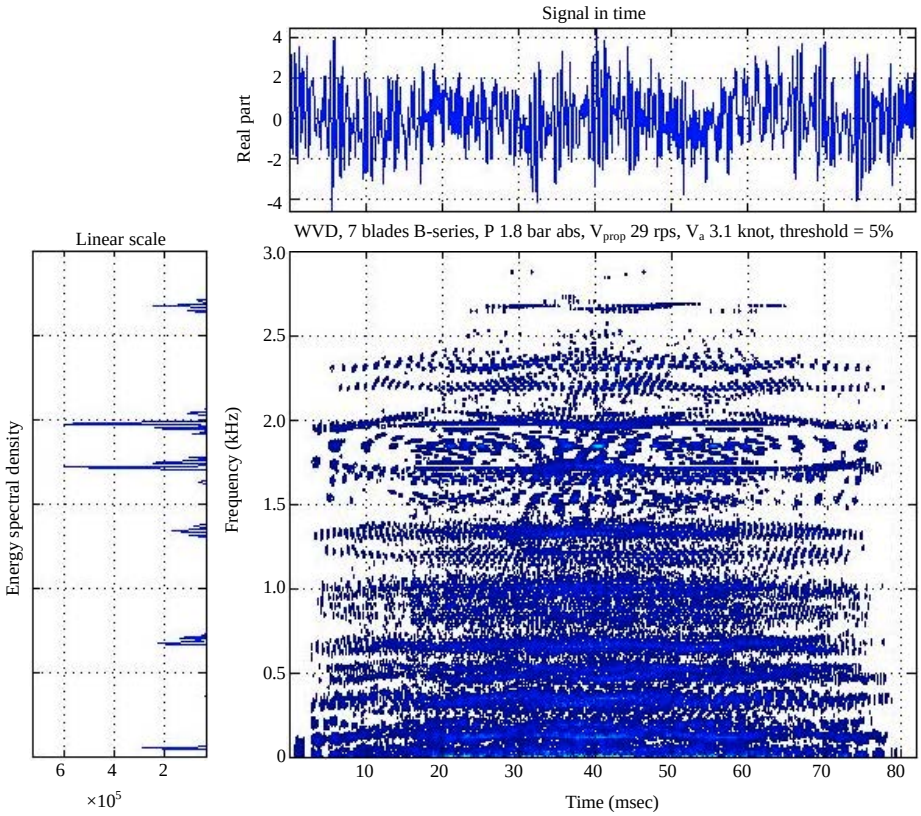

Fig. 17: The WVD representation of the acoustic noise in the tunnel when B-series 7-blade propeller rotates at 29 rps, $V_{water\ in\ the\ tunnel}$ = 3.1 knot and $P_{in\ the\ tunnel}$ = 1.8 bar

Fig. 14b is depicted by the clearer WVD representation at frequencies of about 1.8, 1.3, 0.7 kHz and a few other frequencies below 0.5 kHz. Besides, the ranges of energy in Fig. 14a, b are higher in comparison with the energies in Fig. 15a and b.

Different experiences take place when the propeller cavitation noise originated from the B-series 7-blade propeller is analyzed. There are more frequency components arising in comparison with the propeller cavitation noise of the 4-blade propeller as given in Fig. 14 and 15. However, the energy spectral densities here are lower in comparison with the ones related with the 4-blade propeller cavitation noise. The WVD representations of the cavitation noise in Fig. 16 and 17 show that almost each component is clearly seen at all time and there is no frequency component above 3 kHz.

Figure 16a shows the propeller cavitation noise when only the hub vortex cavitation is present which is similar to the condition given in Fig. 16b. Differences between Fig. 16a and b are that the energy spectral density for 7-blade propeller appears the highest at frequency of 500 Hz while for 4-blade propeller given in Fig. 16b, the highest occurs at 50 Hz. Moreover, similar condition for 4-blade propeller is achieved at the pressure inside the tunnel of 1.8 bar while for 7-blade propeller it is at 1.0 bar.

Figure 16a actually exhibits the WVD representation for 7-blade propeller with the tunnel condition similar to the WVD representation shown in Fig. 14a for 4-blade propeller. However, the type of propeller cavitation noise is similar to the representation given in Fig. 15b. Figure 15b and 16a show the propeller cavitation noise where only the hub vortex cavitation exists. Figure 15 and 16 prove that similar conditions give different representations for two different types of propellers. While the cavitation noise for the 7-blade propeller has more frequency components than those for the 4-blade propeller, the energy spectral density for the 4-blade propeller is higher than that for the 7-blade propeller.

Figure 17 presents the propeller noise for the 7-blade, when no cavitation occurs. There are still some frequency components that appear in this representation, since the acoustic noise is generated not only from the cavitation but also from the motor of the dynamometer, the interaction between the propeller and the water flow, the cooling fan and the impeller of the cavitation tunnel.

Figure 14-17 and the discussion that follows reveal that in any condition with or without cavitations, the noise characteristics caused by 4 and 7-blade propellers are different. This finding indicates the feasibility of using WVD to differentiate propellers with different number of blades based on the noises that they produce.

CONCLUSION

There are three conclusions could be drawn from these experiments described in study as follows: experiment procedure as performed at the IHL cavitation tunnel can be applied to generate propeller cavitations under different pressures, speed of water flow and speed of rotations using two types of B-series propeller. Acoustic noise recorded during the experiment varies based on the environment condition inside the tunnel. This acoustic signal is then analyzed to characterize the propeller cavitation noise.

B-series propeller with 4-blades is easier to produce cavitation than the propeller with 7-blades. As proved during the experiment, there are certain conditions where the 4-blade propeller has already caused the cavitation, the 7-blade propeller has not induced any.

Wigner-Ville distribution is applied for characterizing the propeller cavitation. It can show different representations of the propeller cavitation noise generated by 4 and 7-blade propellers, respectively based on the signal recorded during the experiment in the cavitation tunnel. Further, investigations will be done to identify and classify whether the acoustic signal recorded originated from the 4 or 7-blade propeller.

ACKNOWLEDGEMENT

This research has been funded by the Indonesian Ministry of Research and Technology under the 2011 and 2012 Research Incentive Program.

REFERENCES

Araki, S., K. Yoshinari and A. Shioda, 1982. Measurement of propeller cavitation noise in cavitation tunnel (First report). SRC Technical Note, 10: 18-28 (In Japanese).

Boashash, B., 2003. Time-Frequency Signal Analysis and Processing: A Comprehensive Reference. Elsevier Science, Oxford, pp: 31-38.

Carlton, J., 2007. Marine Propellers and Propulsion. 2nd Edn., Butterworth-Heinemann, Oxford, UK., pp: 249-261.

Collier, R.D., 1997. Ship and Platform Noise, Propeller Noise. In: Encyclopedia of Acoustics, Crocker, M.J. (Eds.). John Wiley and Sons, New York.

Grenie, M., 1990. Acoustic detection of propeller cavitation. Proceedings of International Conference on Acoustics, Speech and Signal Processing, Volume 5, April 3-6, 1990, Albuquerque, NM., USA., pp: 2907-2910.

Park, C., H. Seol, K. Kim and W. Seong, 2009. A study on propeller noise source localization in a cavitation tunnel. Ocean Eng., 36: 754-762.

Ross, D., 1987. Mechanics of Underwater Noise. Pergamon Press, New York, pp: 1-4.

Sharma, S.D., K. Mani and V.H. Arakeri, 1990. Cavitation noise studies on marine propellers. J. Sound Vibration, 138: 255-283.

Widjiati, E., E.B. Djatmiko, W. Wardhana and Wirawan, 2012a. Analysis of propeller cavitation-induced signal using neural network and wigner-ville distribution. Proceedings of OCEANS, 2012 MTS/IEEE, May 21-24, 2012, Yeosu, South Korea, pp: 1-9.

Widjiati, E., E.B. Djatmiko, W. Wardhana and Wirawan, 2012b. Measurement of propeller-induced cavitation noise for ship identification. J. Acoust. Soc. Am., 131: 3489-3489.

Zhang, L., J. Huang and Q. Zhang, 2007. Spectral analysis of noise characteristics caused by ship propeller cavitation. Proceedings of OCEANS 2006-Asia Pasific, May 16-19, 2007, Singapore, pp: 1-5.